



SEISMIC RESPONSE CHARACTERISTICS OF TRADITIONAL WOODEN FRAME BY FULL-SCALE DYNAMIC AND STATIC TESTS

Masaki MAENO¹, Yoshiyuki SUZUKI², Tatsuya OHSITA³ and Akio KITAHARA⁴

SUMMARY

To understand the response characteristics of Japanese traditional wooden structures, shaking table tests and static lateral loading tests were carried out for full-scale models of wooden frames. Dynamic behaviors of the total restoring force, as well as its two major components: one is bending moment resistance from tie beams and another is restoring force due to column rocking, are investigated. Factors possible to affect structure response characteristics are also examined, including tie beams and angle ties. It is found that when the structure deformation is small, the restoring force due to column rocking is the major part of the total restoring force. With the deformation increasing, the bending moments from tie beams become predominant. The axial force acting on the column has little influence on the bending moment resistance of tie beams, but it affects significantly the restoring force due to column rocking.

INTRODUCTION

Traditional wooden structures in Japan, such as temples and shrines, have been built by using typical wooden character traits integrated together. Thick columns, joints of column-tie beams, and bracket complexes are typical examples of the character traits used by Japanese skilled carpenters for a long time. However, structural mechanisms of these wooden structures have yet known because of complexity of these timberworks and uncertainties of timber mechanical properties. For the purpose of disaster prevention and seismic design, it is desirable to understand and analyze their static and dynamic behaviors qualitatively and quantitatively.

In a traditional wooden structure, thick columns and beams used to tie columns are the most important structural elements. The columns are set on top of base stones, but not fixed with them. At the top of columns are bracket complexes to support the heavy roof. When the structure deforms during earthquakes, the columns are rocking, and embedment at the top and bottom of the columns creates restoring moments. Beams are used to tie the columns together at several levels of height using mortises and tenons joints or double notched joints without steel nails. When the structure deforms during earthquakes, embedment in

¹ Graduate School of Engineering, Kyoto University, Japan, maeno@zeisei.dpri.kyoto-u.ac.jp

² Disaster Prevention Research Institute, Kyoto University, Japan, Suzuki@zeisei.dpri.kyoto-u.ac.jp

³ J-Home Corp., Japan, tatuya-o@po.incl.ne.jp

⁴ Tottori University of Environmental Studies, Japan, kitahara@kankyo-u.ac.jp

joints takes place, and generates forces and moments in all jointing members. The static characteristics of these structural elements have been investigated experimentally and theoretically [1-4]. To assess the seismic performance, shaking table tests and static lateral loading tests were carried out on full-scale models of traditional wooden frames [5-7].

It is known that the restoring force of a wooden structure during its deformation is a result of all bending moments at the top and bottom of columns due to rocking, as well as those at column-beam joints due to resistance of tie beams. However, quantitative descriptions have yet established, and several factors possible to affect structure response characteristics need to be examined. The present study tends to solve these problems through dynamic and static tests on full-scale models. By analyzing the test data, quantitative behaviors of the total restoring force and its two parts: bending moments from tie beams and restoring force due to column rocking will be evaluated. Effects of tie beams, angle ties and roof weight on structure dynamic properties will be assessed.

STRUCTURE OF TRADITIONAL WOODEN BUILDINGS

Japanese wooden buildings possess a typical structure consisting of several major elements, as shown in Fig. 1 and described below.

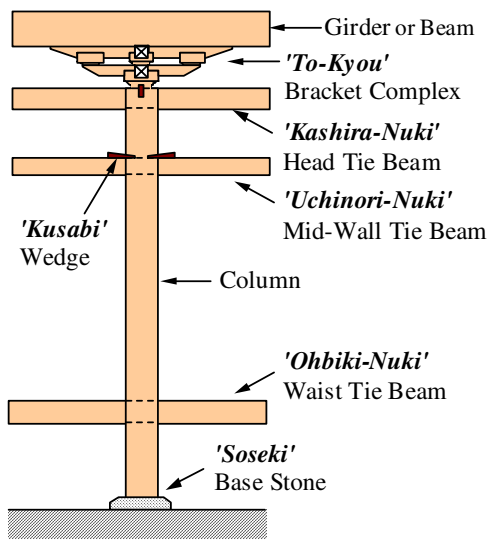


Fig. 1 Structural elements of Japanese traditional wooden buildings

(1) Bracket complex at the top of column (*To-Kyou*)

A bracket complex consists of rectangular layers of blocks and bracket arms with dowels. The embedment and friction inside the bracket complex and between the column top and the bracket complex during column rocking generate forces and moments, which contribute to the total restoring force of the structure.

(2) Joints of column- tie beam (*Nuki*)

Columns are tied together by penetrating tie beams at waist height, at mid-wall height and at head of columns. Because the columns and the tie beams are connected with each other using mortise and tenon joints or double notched joints without steel nails, embedment and friction at the joints occur during earthquakes, and generated bending moments contributing to the total restoring force.

(3) Column base

Thick columns are set on top of base stones, but not fixed with them. During earthquakes, the columns are rocking, and embedment between column bottoms and base stones produces moments, which resist the column inclination and also contribute to the total restoring force.

According to the above analysis, the total restoring force of a wooden structure has two different types of sources: one is the resistant bending moments from the tie beams and another is the restoring moments at the top and bottom due to column rocking. The nature and properties of the restoring force, as well as its two types of sources will be investigated.

SHAKING TABLE TESTS AND STATIC LATERAL LOADING TESTS

Shaking table tests and static lateral loading tests were carried out on full-scale models of wooden frames in Disaster Prevention Research Institute, Kyoto University. In the tests, strains at various locations were

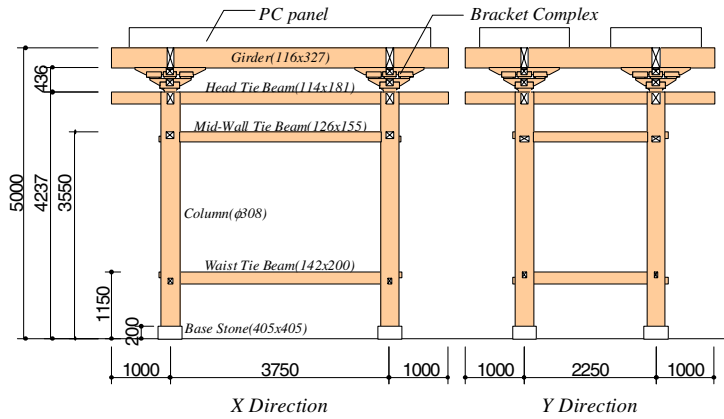


Fig. 2 Specimen A (unit: mm)



Fig. 3 Full-scale model in shaking table tests

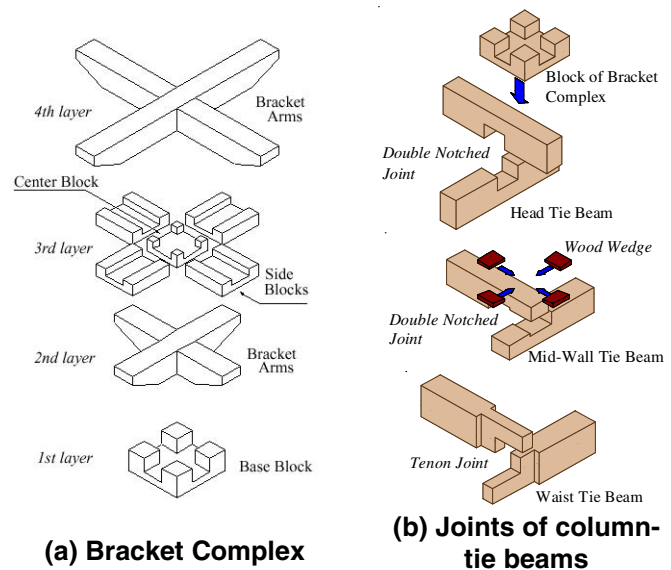
measured, and the measured strains were used to calculate bending moments at column-beam joints according to the stress-strain relationship and the mechanics of materials.

Outline of shaking table tests

For different test purposes, several full-scale models of Japanese traditional wooden frames were built with slightly different structures. Specimen A was a complete model consisting of four circular columns, waist tie beams, mid-wall tie beams, head tie beams, bracket complexes, girders and PC panels, as shown in Figs. 2 and 3. The size of the specimen was: 3.75m in X-direction, 2.25m in Y-direction, and 5.0m in height. Each column was about 4.24m in height and 0.308m in diameter. As for the materials, the columns and the wedges at the joints of column-mid-wall tie beam were made of Japanese cypress, the bracket complexes of Afrormosia (Assamela), and the other parts of Douglas fir. The columns were set on base stones without protruding pins. Bracket complexes were on the top of the columns, and supported the roof through girders. Either the head tie beams or the mid-wall tie beams were connected with each other using double notched joints into mortises of columns. The waist tie beams were connected using tenons into mortises of columns. Fig. 4 shows details of the bracket complex and different joints of column-tie beam.

Angle ties in the level of the waist tie beams, head tie beams and girders were added to reduce torsion of the structure and to enhance the stiffness in horizontal directions. Two PC panels were fastened to the girders, which had a total weight of about 110kN (equivalent to the weight of a typical roof) and provide axial forces to the columns.

To compare seismic performances between different structures, three models: specimens B, C, and D were constructed from specimen A by removing different parts. In specimen B, the angle ties at the level of the waist tie beams were removed as shown in Fig. 5. In specimen C, the mid-wall tie beams were removed as shown in Fig. 6. Specimen D is the weakest one in which the mid-wall tie beams, the waist tie beams in X-direction, and the angle ties at the level of the waist tie beams were removed, as shown in Fig. 7. By



(a) Bracket Complex

(b) Joints of column-tie beams

Fig. 4 Details of bracket complex and joints of column-tie beams

comparing test results of specimens A, B, C and D, effects of the tie beams and angle ties can be assessed. In the shaking table tests, accelerometers were installed on the top of the PC panels, and the measured accelerations were used to calculate restoring forces of the specimens. In the tests on specimens A, B and C, recorded ground accelerations of El Centro 1940 NS were used as input to the shaking table in X-direction. For specimen D, sinusoidal accelerations were the input in X-direction. To obtain natural frequencies of the specimens, sweeping sinusoidal waves were used as input.

Outline of static lateral loading tests

In static tests, only specimen D was used in order to show the contribution from the column rocking to the restoring force more clearly. The lateral force was applied at the PC panels in X-direction with the control quantity being the displacement. A load cell was installed between the actuator and the PC panels to measure the restoring forces of the specimens, as shown in Fig. 8. As for the axial force in the columns, two cases were tested: one is the same as that in the shaking table tests, i.e., using two PC panels with a total weight of 110kN, and another is two PC panels and four steel panels with a total weight of 190.3kN.

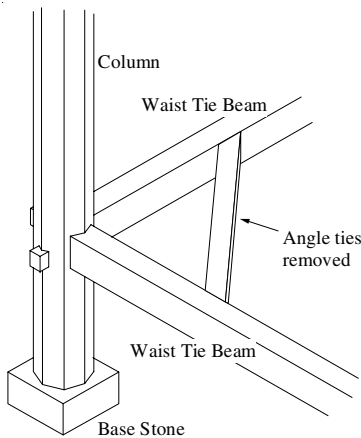


Fig. 5 specimen B (unit: mm)

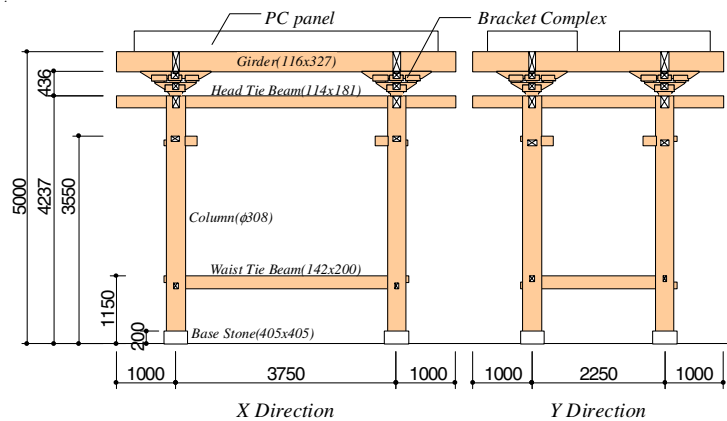


Fig. 6 Specimen C (unit: mm)

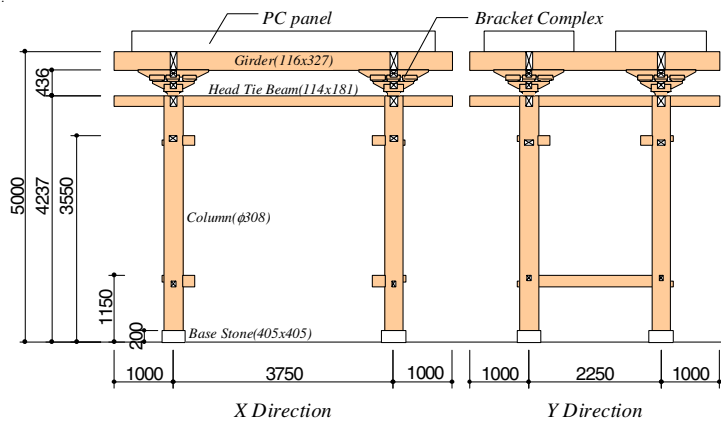


Fig. 7 Specimen D (unit: mm)

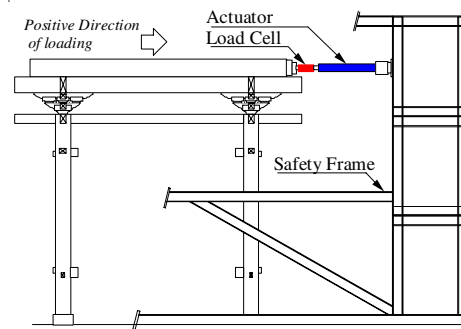


Fig. 8 Loading and measuring methods in static tests on specimen D

NATURAL FREQUENCIES OF TEST SPECIMENS

For designing the tests, it was beneficial if some dynamic characteristics of the specimens had been known. One of the characteristics, the natural frequency, was relatively easy to obtain. Therefore, before the tests, micro-tremor measurements and vibration tests using sweeping sinusoidal waves were carried out on specimens A, B and C to obtain the natural frequencies of the specimens. For specimen D, the micro-tremor measurements and the vibration test in Y direction were not performed due to safety concern. In the micro-tremor measurements, speedometers were installed at the tops of the shaking table and the PC panels, and the measured velocities were used to calculate velocity transfer functions using Fourier transform. In the vibration tests, accelerometers were installed at the tops of the shaking table and the PC panels, and the measured accelerations were used to calculate acceleration transfer functions. The peak location of each transfer function is the fundamental frequency of the corresponding specimen. We called this fundamental frequency as the natural frequency of the structure. Since the structures suffered from large deformation repeatedly in the shaking table tests and static tests, the same micro-tremor measurements were conducted again to determine the effect of repeated large deformations on the structure dynamic characteristics.

Micro-tremor measurements

Micro-tremor measurements were carried out for specimen A, B, and C to compare the natural frequencies before and after the specimens experienced deformations through the shaking table tests and the static tests. Table 1 lists the natural frequencies of specimens A, B and C. It should be mentioned that the natural frequency (1.26Hz) of specimen A in X-direction prior to the tests was measured immediately after the specimen was constructed. Thus all joints were very tight. This was the reason for a large decrease after the tests (from 1.26Hz to 1.15Hz). For specimens B and C, no significant changes were observed. There was almost no change in Y-direction since tests were carried out mainly in X-direction. It should be pointed out that the deformations were quite small in micro-tremor measurements. Thus, it is reasonable to say that the tests did not change the structure natural frequency in the range of small deformations.

Table 1 Natural frequencies from micro-tremor measurements before and after the tests (unit: Hz)

Specimen	before or after tests	X Direction	Y Direction
A	before	1.26	1.29
	after	1.15	1.29
B	before	1.12	1.29
	after	1.11	1.28
C	before	1.10	1.17
	after	1.11	1.17

Vibration tests using sweep sinusoidal waves

Vibration tests using sweeping sinusoidal waves were carried out for specimen A, B, C and D before the shaking table tests and static tests. The vibration tests were not performed after the tests. Table 2 lists the results. The natural frequencies reduced substantially from specimens A to D, indicating the effects of the angle ties, the mid-wall tie beams and the waist tie beams on the structure stiffness are significant.

Table 2 Natural frequencies from vibration tests using sweep sinusoidal waves before the tests (unit: Hz)

Specimen	X Direction	Y Direction
A	0.87	0.84
B	0.77	0.79
C	0.66	0.76
D	0.50	-

RESTORING FORCE CHARACTERISTICS

Shaking table tests were carried out for specimen A, B and C to obtain restoring force characteristics. To obtain hysteresis loops of the restoring forces, an El Centro NS wave scaled up to a maximum acceleration of 200cm/s^2 (called "El Centro NS 200cm/s^2 " hereafter) was used as the input excitation. Skeleton curves

of the restoring forces were also obtained with El Centro NS waves of maximum accelerations between 50cm/s^2 and 200cm/s^2 as input.

Restoring forces

Figs. 9(a) and 9(b) show hysteresis loops and skeleton curves, respectively, for the total restoring forces of specimens A, B and C in X-direction. Two important features can be observed from the figures. The hysteresis loops for each specimen overlap each other, indicating stable hysteretic restoring force characteristics of the wooden structures. Secondly, the slope of the restoring force tends to be lower for an increasing deformation angle, namely, the stiffness of the structure is decreasing, called softening stiffness.

As expected, the stiffness of specimen A is the highest since both specimens B and C are weaker than A by removing some parts. The fact that the stiffness of specimen C is lower than that of specimen B indicates that the mid-wall tie beams provide stronger support to the structure than the angle ties at the waist tie beam level.

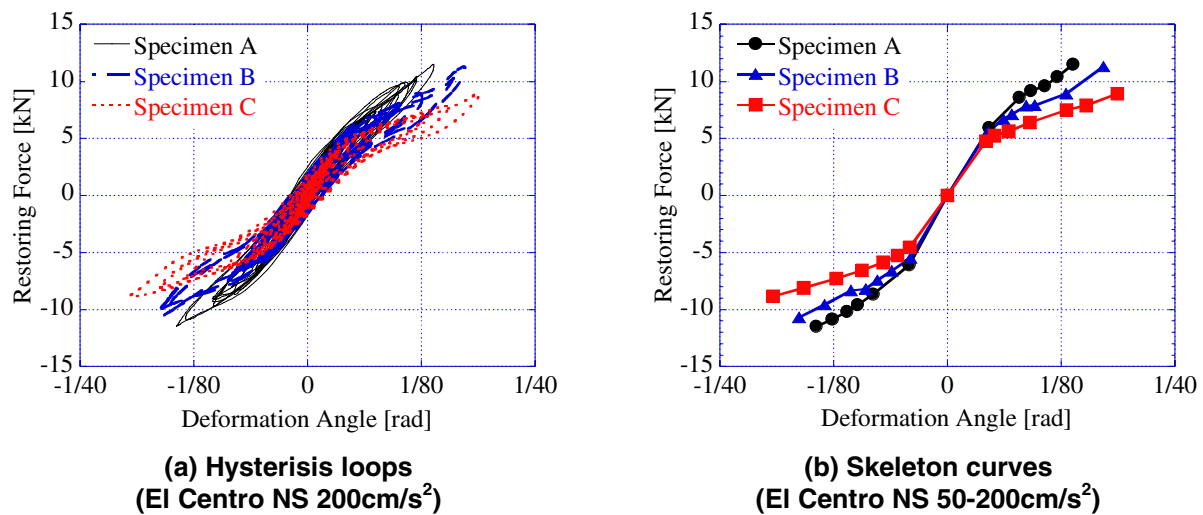


Fig. 9 Total restoring forces of specimen A, B and C in X-direction (shaking table tests)

Equivalent natural frequencies based on the restoring forces

For a system with a nonlinear restoring force, the natural frequency of the system varies with the amplitude. For a given amplitude, the equivalent natural frequency is defined as the natural frequency of the corresponding linear system which has the same maximum restoring force as that of the nonlinear system. Although the equivalent natural frequency does not have an explicit physical meaning, it gives a general trend as how the system natural frequency changes with the amplitude. Fig. 10 depicts the calculated equivalent natural frequencies in X direction for specimen A, B and C. As expected, the equivalent natural frequencies of specimen A are the highest, those of specimen C are the lowest at the same deformation angle. They are decreasing with an increasing deformation because of the softening nature of the stiffness. As the deformation is very small, they tend to converge

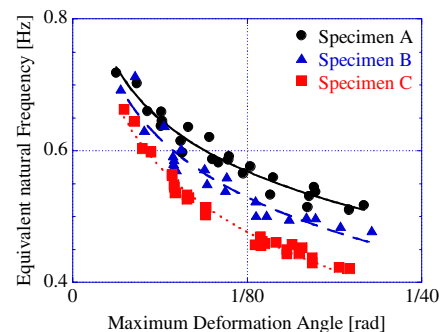


Fig. 10 Equivalent natural frequency by the maximum restoring force of hysteretic loops (specimen A-C)

since effects from the tie beams and angle ties are insignificant. On the other hand, the differences increase with an increasing deformation, in which case the effects of the tie beams and angle ties become more significant.

MOMENT RESISTANCE AT COLUMN-BEAM JOINTS

In the above shaking table tests carried out for specimen A, B and C using El Centro NS as input in X-direction, the bending moments at the joints of column-tie beams were obtained simultaneously. In calculating these moments from measured strain data, the Young's modulus was 9.12kN/mm^2 for the head tie beams, 10.52kN/mm^2 for the mid-wall tie beams, and 10.71kN/mm^2 for the waist tie beams, obtained from material tests.

Figs. 11 through 13 show the relations of the bending moment and beam rotational angle at the joints of column and three types of tie beams, respectively. For each joint, both hysteresis loops and skeleton curves are depicted. It should be pointed out that only specimens A and B are listed in Figs. 12(a) and 12(b) since the mid-wall tie beams were removed.

It is found that the hysteresis loops and skeleton curves are asymmetric for the joint of column-head tie beam, but they are symmetric for the other two joints. This is because the embedment occurs asymmetrically at the joint of column-head tie beam, but symmetrically at the other joints, as shown in Figs. 14(a) and 14(b).

All these figures show that the rotational stiffness of each column-beam joint is the highest in specimen A.

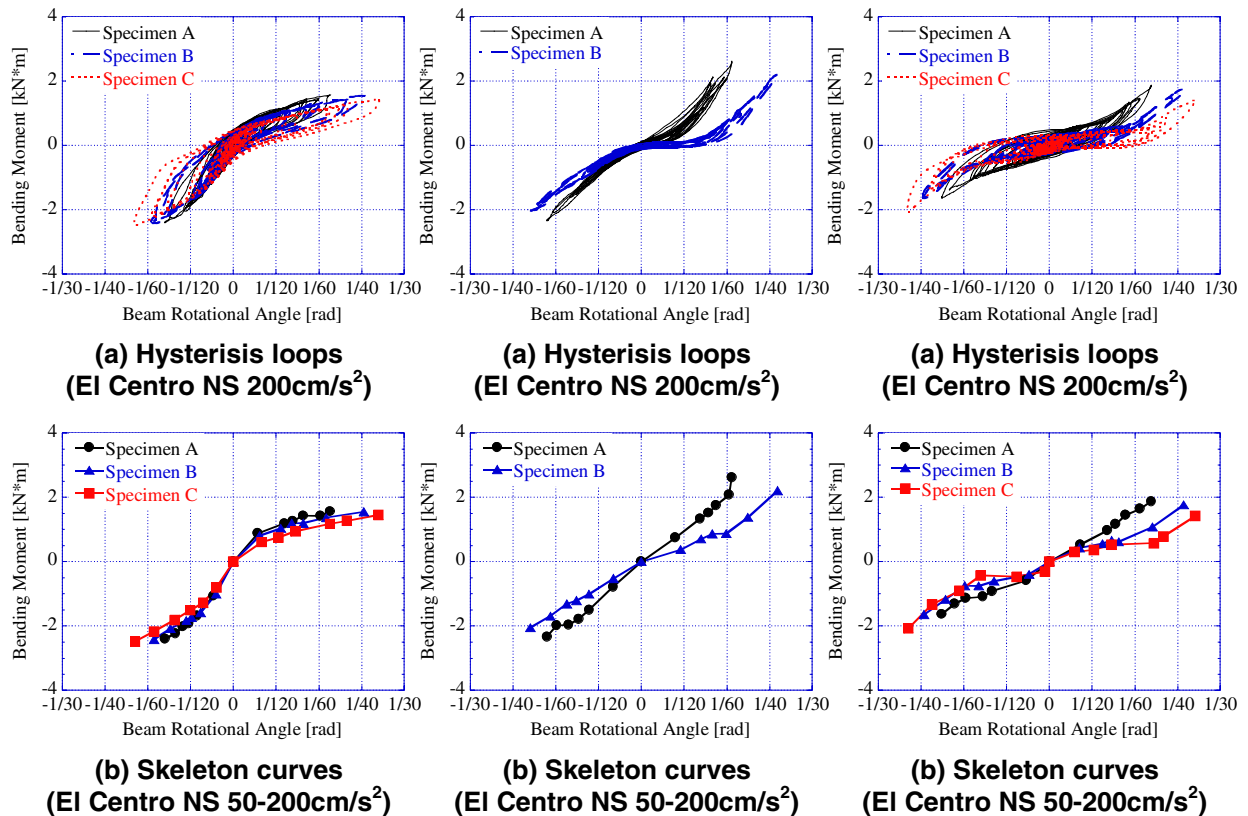


Fig. 11 Moment-rotation relationship at the joint of column-head tie beam (shaking table tests)

Fig. 12 Moment-rotation relationship at the joint of column-mid-wall tie beam (shaking table tests)

Fig. 13 Moment-rotation relationship at the joint of column-waist tie beam (shaking table tests)

This may be caused by two factors. One is because specimen A has the highest stiffness. It distributes to all contributing resisting moments to different extents. Another may be due to the plastic deformations in the specimens since specimen A was tested first.

Figs. 12(a) shows slip-shaped hysteresis loops for the bending moments at the joint of column-mid-wall tie beam, and shows a higher rotational stiffness than those at the other two joints. This can be explained by the special structure of the joint. The mid-wall tie beams were connected using double notched joints with wood wedges, while either the head tie beams or the waist tie beams were connected without wood wedges. These wedges resulted in a higher stiffness. However, the area of the hysteresis loops at the joint was smaller than those at the other joints, indicating a lower ability of energy dissipation.

The moment-rotation relationship at the joint of column-waist tie beam also shows slip-shaped hysteresis loops, as seen in Fig. 13(a). It is found that the rotational stiffness at the joint is lower than those at the other two joints. This is also caused by the different structure of the joint. The waist tie beams were connected together only using tenons without engagement in X and Y directions, while the other tie beams were connected together in both X and Y direction using double notched joints. This resulted in more slipping occurring at the joint than those at the other joints.

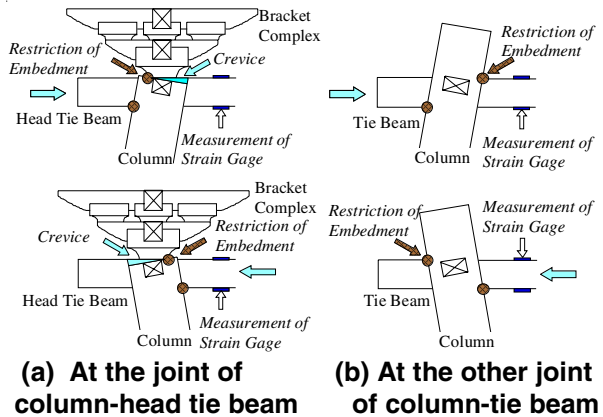


Fig. 14 Embedment and crevice occurring at the joints of column-tie beam

COMPARISON OF RESULTS FROM SHAKING TABLE TESTS AND STATIC TESTS

Both static lateral loading tests and shaking table tests were carried out on specimen D in which the mid-wall tie beams and waist tie beams were removed. In the static tests, the maximum displacement applied at the top of the specimen was 120mm, and in the shaking table tests, the input acceleration was sinusoidal 0.60Hz 35cm/s². Fig. 15 depicts the restoring forces of specimen D. The results obtained from the two types of tests are almost identical. Fig. 16 shows the bending moments at the joint of column-head tie beam. The results from the static tests and shaking table tests are of similar characteristics, except the rotation stiffness obtained from the static tests is slightly higher than that from the shaking table tests in the range of a positive rotational angle. It is probably related to the asymmetric behavior of the joint embedment.

COMPARISON OF RESULTS FOR TWO DIFFERENT ROOF WEIGHTS

To assess the influence of the roof weight, static tests were performed on specimen D under two different conditions: one with two PC panels of a total weight of 110kN, and another with four additional steel panels of a total weight of 190.3kN. For the two cases, the maximum displacements applied at the top of the specimen were 140mm and 155mm, respectively. Fig. 17 and 18 depict the restoring force and the bending moments at the joint of column-head tie beam, respectively, for the two cases. Fig. 18 shows that the axial force in the column does not have effect on the bending moment resistance of the tie beams, while Fig. 17 clearly indicates that the restoring force increases significantly in the case of the heavier roof. The increase in the present case is about 33%.

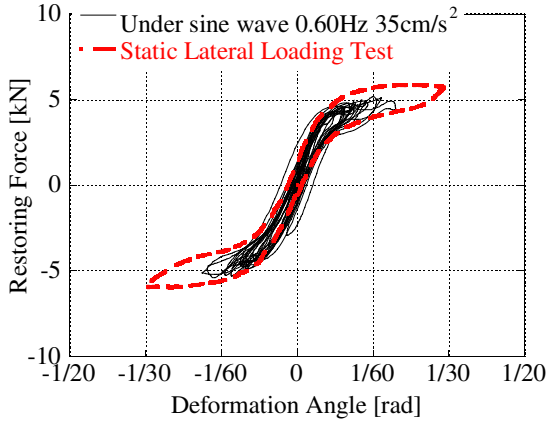


Fig. 15 Comparison between restoring forces from shaking table tests and static lateral loading tests

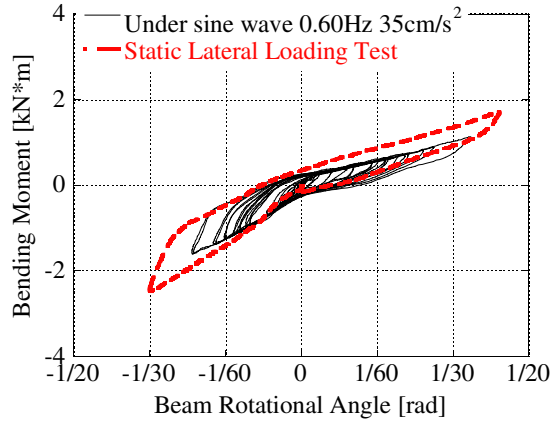


Fig. 16 Comparison between bending moments from shaking table tests and static lateral loading tests at the column-head tie beam joint

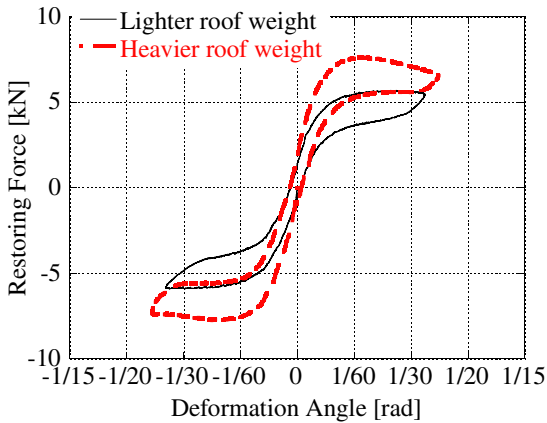


Fig. 17 Comparison between restoring forces under different roof weights (static tests)

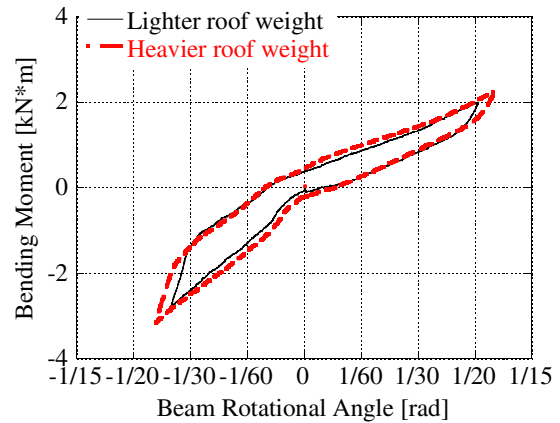


Fig. 18 Comparison between bending moments under different roof weights at column-head tie beam joint (static tests)

It is understood that the bending moments from the tie beams depend on the column-beam joint structure and the column rotational angle, and they should not be influenced by the axial force in the column. On the other hand, a heavier roof enhances the restoring moments at the top and bottom of column due to column rocking; therefore, increasing the total restoring force.

EVALUATION OF RESTORING FORCES DUE TO COLUMN ROCKING

As shown in the previous section, the restoring moments at the top and bottom of the column due to column rocking contribute significantly to the total restoring force. To evaluate the component in the total restoring force due to column rocking, the tie beams should be removed as many as possible. Specimen D was constructed for this purpose. The head tie beams still remained to keep the structure stable. According to the equilibrium condition of specimen D, we have

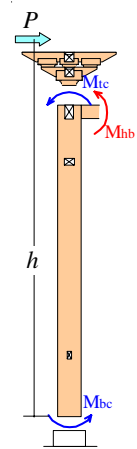
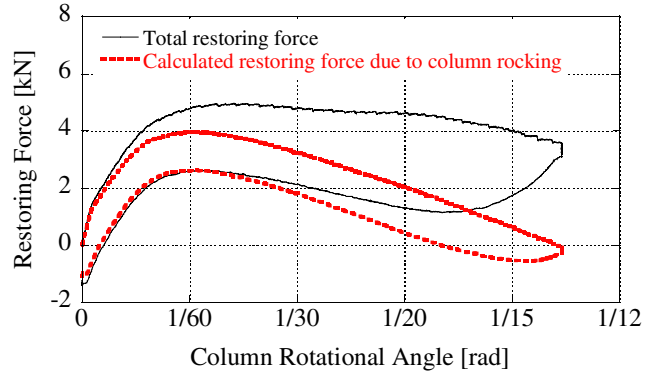


Fig. 19 Moment equilibrium of column

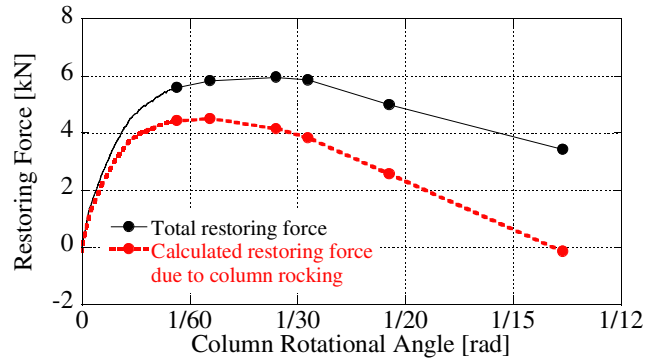
$$Ph = M_{tc} + M_{bc} + M_{hb} = M_{rc} + M_{hb} \quad (1)$$

where, as shown in Fig. 19, P is the horizontal force at the top of the specimen, h is the height from the ground to the actuator, M_{tc} and M_{bc} are the total bending moment at the tops and bottoms of all columns, respectively, M_{hb} is the total bending moment at all joints of column-head tie beam, and $M_{rc} (= M_{tc} + M_{bc}) = Ph - M_{hb}$ is the restoring moment due to rocking. Since the total restoring force P and the moment M_{hb} can be measured, the restoring moment M_{rc} can be calculated from Eq. (1). The force M_{rc}/h is called as "the restoring force due to column rocking" as more fully discussed hereinafter.

The same static tests were carried out for specimen D only in one direction of loading with 300mm as the maximum controlling displacement. The measured total restoring force and the restoring force due to rocking calculated from Eq. (1) are shown in Fig. 20(a) for hysteresis loops and in Fig. 20(b) for skeleton curves. It is seen from the figures that for small deformation angles, main portion of the total restoring force is from rocking since a small column deformation implies a small deformation of a tie beam, and induces a low resistant bending moment from the beam. With deformation increasing, contributions from the tie beams increase and from column rocking reduce. At a large deformation angle above 1/15 radian, the restoring force due to rocking was negative. However, in the tests, specimen D still maintained enough strength to prevent it from collapsing since the total restoring force was still positive due to the large resisting bending moments from the head tie beams. That is the reason why traditional wooden structures have high deformability.



(a) Hysteresis loops



(b) Skeleton curves

Fig. 20 The total restoring force and the restoring force due to column rocking (static tests)

CONCLUSION

The results from the shaking table tests and the static lateral loading tests on full-scale models of Japanese traditional wooden frames have been analyzed in the paper, and the following conclusion can be drawn:

- (1) The restoring force of a wooden structure consists of two parts: one is the resistant bending moments from the tie beams and another is the restoring forces at the column top and bottom due to rocking. When the deformation is small, the restoring force due to column rocking is the major part of the total restoring force. With the deformation increasing, the bending moments from the tie beams become more important.

- (2) When the structure deformation is large, the bending moment resistance from the tie beams is predominant in the total structure restoring force. It is this resistance that allows large deformations of wooden structures and prevents many of them from collapsing.
- (3) The total restoring force of a wooden structure exhibits a stable behavior. It is hysteretic and dissipating energy, and it is also softening with a decreasing slope (i.e. stiffness) for an increasing deformation.
- (4) The tie beams and angle ties have significant effects on the structure stiffness and natural frequency, especially when the structure deformation is large.
- (5) The axial force in columns, depending mainly on the roof weight, has little influence on the bending moment resistance of the tie beams, but it affects significantly the restoring force due to rocking. A heavier roof causes a larger restoring force due to column rocking.

ACKNOWLEDGEMENTS

This research was partially supported by Grant-in-Aid for Scientific Research (A) under Grant No. 13305036, from the Ministry of Education, Culture, Sports, Science and Technology. The authors are grateful to Prof. K. Komatsu, Dr. S. Takino, and Dr. T. Mori of Wood Research Institute, Kyoto University for carrying out material tests, and to Mr. N. Ichikawa and Dr. H. Shimizu of Disaster Prevention Research Institute, Kyoto University for their helps in shaking table tests and static tests. Valuable advice from Prof. G. Q. Cai of Florida Atlantic University is also appreciated.

REFERENCES

1. Ban S., "Mechanical Study on the Japanese Traditional Frame", *Transactions of Architectural Institute of Japan*, 1941.4, pp252-258 (in Japanese)
2. Kawai N., "Column Rocking Resistance in Japanese Traditional Timber Buildings", *Proc. of the International Engineering Conference*, Vol.1, 1996.10, pp186-190
3. Gotoh K., "Research on the Wooden Semi-Rigid Frame (Nuki Structure)", *Journal of Structural and Construction Engineering, Transactions of Architectural Institute of Japan*, No.366, 1986.8, pp119-125 (in Japanese)
4. Fujita K., Kimura M., Ohashi Y., and Sakamoto I., "Hysteresis Model and Stiffness Evaluation of Bracket Complexes Used in Traditional Timber Structures Based on Static Lateral Loading Tests", *Journal of Structural and Construction Engineering, Transactions of Architectural Institute of Japan*, No.543, 2001.5, pp121-127 (in Japanese)
5. Suzuki Y., Katagihara K. Iwasa Y., Takata K., Yamamoto M., Goto M., and Kitahara A., "Dynamic Characteristics and Seismic Performance of Traditional Wooden Structure by Shaking Table Tests", *Proceedings of U.S.-Japan Joint Workshop and Third Grantees Meeting U.S.-Japan Cooperative Research in Urban Earthquake Disaster Mitigation*, Seattle, USA, 2001.8, pp328-337
6. Katagihara K., Suzuki Y., Goto M., Kitahara A., and Iwasa Y., "A Study on Dynamic Performance and Seismic Strengthening of the Traditional Wooden Structure in Japan", *IABSE Conference Innovative Wooden Structures and Bridges*, Lahti, Finland, 2001.8
7. Suzuki Y., Maeno M., Saito S., Kitahara A., Gotou M., Suda T., and Ohshita T., "Full-Scale Dynamic and Static Tests of Traditional Wooden Frame", *Journal of Structural and Construction Engineering, Transactions of Architectural Institute of Japan*, No.574, 2003.12, pp135-142 (in Japanese)